Neurotrophically Induced Mesenchymal Progenitor Cells Derived from Induced Pluripotent Stem Cells Enhance Neuritogenesis via Neurotrophin and Cytokine Production

RACHEL M. BRICK,[a,b] AARON X. SUN,[a,c] ROCKY S. TUAN [ID][a,b,c]

[a]Center for Cellular and Molecular Engineering, Department of Orthopaedic Surgery, University of Pittsburgh School of Medicine, Pittsburgh, Pennsylvania, USA; [b]Department of Pathology, University of Pittsburgh School of Medicine, Pittsburgh, Pennsylvania, USA; [c]Department of Bioengineering, University of Pittsburgh Swanson School of Engineering, Pittsburgh, Pennsylvania, USA

Correspondence: Rocky S. Tuan, Ph.D., Center for Cellular and Molecular Engineering, Department of Orthopaedic Surgery, University of Pittsburgh School of Medicine, 450 Technology Drive, Room 221, Pittsburgh, Pennsylvania 15219, USA. Telephone: 1 4126482603; e-mail: rst13@pitt.edu

ABSTRACT

Adult tissue-derived mesenchymal stem cells (MSCs) are known to produce a number of bioactive factors, including neurotrophic growth factors, capable of supporting and improving nerve regeneration. However, with a finite culture expansion capacity, MSCs are inherently limited in their lifespan and use. We examined here the potential utility of an alternative, mesenchymal-like cell source, derived from induced pluripotent stem cells, termed induced mesenchymal progenitor cells (MiMPCs). We found that several genes were upregulated and proteins were produced in MiMPCs that matched those previously reported for MSCs. Like MSCs, the MiMPCs secreted various neurotrophic and neuroprotective factors, including brain-derived neurotrophic factor (BDNF), interleukin-6 (IL-6), leukemia inhibitory factor (LIF), osteopontin, and osteonectin, and promoted neurite outgrowth in chick embryonic dorsal root ganglia (DRG) cultures compared with control cultures. Cotreatment with a pharmacological Trk-receptor inhibitor did not result in significant decrease in MiMPC-induced neurite outgrowth, which was however inhibited upon Jak/STAT3 blockade. These findings suggest that the MiMPC induction of DRG neurite outgrowth is unlikely to be solely dependent on BDNF, but instead Jak/STAT3 activation by IL-6 and/or LIF is likely to be critical neurotrophic signaling pathways of the MiMPC secretome. Taken together, these findings suggest MiMPCs as a renewable, candidate source of therapeutic cells and a potential alternative to MSCs for peripheral nerve repair, in view of their ability to promote nerve growth by producing many of the same growth factors and cytokines as Schwann cells and signaling through critical neurotrophic pathways. STEM CELLS TRANSLATIONAL MEDICINE 2018;7:45–58

SIGNIFICANCE STATEMENT

Using human induced pluripotent stem cells, progenitor cells that resemble adult tissue-derived mesenchymal stem cells, which are currently considered to be a promising cell type for regenerative therapies, have been derived. In addition to exhibiting similar surface markers and morphology, these cells secrete factors into their conditioned medium that are capable of promoting neurite sprouting and axon elongation in an embryonic dorsal root ganglion explant culture model. Given the indefinite life span of induced pluripotent stem cells, the findings of this study strongly suggest their utility as a source of neurotrophic cells that may be applied for nerve regeneration and repair.

INTRODUCTION

Peripheral nerve damage often accompanies and complicates limb injuries. Proper healing of nerve damage can be quite challenging, especially as the success of nerve regeneration is dependent upon the rate and quality of axon growth and myelination to bridge the gap across the injured area. Regeneration is mediated by Schwann cells, which secrete neurotrophic factors and migrate to form Bands of Büngner, a longitudinal tunnel that both guides the regenerating neuron toward its target and secretes neurotrophic factors to encourage nerve regrowth. However, this process is error-prone, and can often result in formation of painful neuromas. Currently, the gold standard treatment for peripheral nerve repair is a direct end-to-end suture. In the case of longer gaps where tension-less end-to-end sutures cannot be achieved, autologous nerve graft surgery at the sacrifice of other nerves from a donor site deemed less important is carried out [1]. However, the best treatment is

still limited, that is, even with multiple surgeries and meticulous care to align fascicles and match graft and host nerve sizes, complete motor function is often never fully regained, and may also leave the donor site at least partially deinnervated [2].

An alternative to the autologous nerve graft is an autologous Schwann cell transplant to the injured site. While this method does not sacrifice a healthy nerve, it still risks damage to the nerve at the Schwann cell donor site. The patient thus risks similar donor site morbidities as those seen in autologous nerve grafts. Allogeneic Schwann cell transplants have also been attempted, but due to the immunogenic nature of Schwann cells, these transplants are quickly rejected by the host [3]. Because of these limitations, a more practical approach is needed. To address this need, several studies have shown that bone marrow-derived mesenchymal stem cells (MSCs) have the ability to act as Schwann-like cells, given the proper induction environment, and can support nerve regeneration by secreting neurotrophic factors (NTFs) [4, 5].

While neurotrophically induced-MSCs (NI-MSCs) are capable of producing many of the same NTFs as Schwann cells, they have finite expansion capacity, and require invasive techniques to acquire, for example, bone marrow aspiration. Induced pluripotent stem cells (iPSCs), derived by reprogramming adult somatic cells, including MSCs, that exhibit embryonic stem cell (ESC)-like pluripotency, represent a potential cell source that can overcome this drawback. iPSCs are produced by reprogramming with four transcription factors and have a virtually unlimited expansion capacity. We have shown that after expansion, the iPSCs can be differentiated into MSC-like cells, which we have termed induced mesenchymal progenitor cells (MiMPCs) [6]. In this manner, this technology has the potential to yield an almost unlimited supply of MiMPCs. In this study, we aim to test if these MiMPCs, originally derived from MSCs, have the same ability to support neuronal regeneration as the parent MSC. With this capacity, MiMPCs may represent a potentially infinitely renewable cell source for the support of nerve regeneration and cell therapy. Our results reported here show that MiMPCs can secrete NTFs after neuroinductive treatment, and can produce factors to improve neurite outgrowth in vitro in a chick embryonic dorsal root ganglion (DRG) model. These findings suggest that neurotrophically induced-MiMPCs (NI-MiMPCs) may be considered a suitable substitute cell type to support nerve growth.

MATERIALS AND METHODS

Generation of MiMPCs from iPSCs

A previously reported human iPSC line derived from reprogramming of human adult bone marrow MSCs was used [6]. Feeder-free, undifferentiated iPSCs colonies were grown to confluency in six-well plates coated with Matrigel (Corning, Corning, NY), using mTesR1 media (Stem Cell Technologies, Vancouver, Canada). Confluent iPSC colonies are switched from mTeSR1 media to MSC growth medium (GM), consisting of α-MEM (ThermoFisher, Waltham, MA), supplemented with 10% fetal bovine serum (FBS; ThermoFisher), 1 ng/ml fibroblast growth factor-2 (FGF2; RayBiotech, Norcross, GA), and antibiotic-antimycotic (penicillin-streptomycin/fungizone [PSF]; ThermoFisher). The iPSCs are maintained in the MSC growth medium for 7 days with medium changes every 2 to 3 days. After 1 week, cells are trypsinized and seeded into gelatin (Stem Cell Technologies, Vancouver, Canada) coated flasks for continued culture.

Neurotrophic Induction and Preparation of Conditioned Media

MiMPCs and control MSCs were plated at approximately 3,000 cells per cm² on gelatin-coated flasks and maintained in MSC GM until the cultures reached 70% confluency. Prior to culture in neurotrophic induction medium (NIM), cells were pretreated for a total of 72 hours: the first 24 hours with pretreatment medium consisting of α-MEM supplemented with 10% FBS, 1 mM β-mercaptoethanol (Sigma-Aldrich, St. Louis, MO), and PSF, and the following 48 hours of pretreatment included 35 ng/ml retinoic acid (RA; Sigma-Aldrich) in the pretreatment medium. For 7 days following pretreatment, MiMPCs and control MSCs were treated with NIM, consisting of Dulbecco's MEM (DMEM)/Ham's F-12 medium (ThermoFisher) supplemented with 5% FBS, 0.5 mM 3-isobutyl-1-methylxanthine (Sigma-Aldrich), 5 ng/ml platelet-derived growth factor (Peprotech, Rocky Hill, NJ), 50 ng/ml recombinant human neuregulin (hNRG1; R&D Systems, Minneapolis, MN), 10 ng/ml FGF2, 20 ng/ml epidermal growth factor (EGF; Peprotech), 6 µg/ml RA, 10 ng/ml IL-1β, and 2% vol/vol B-27 Supplement (ThermoFisher). The MiMPCs and MSCs remained in NIM medium for 7 days, with one intermittent medium change after 3 days in culture. After the 7-day induction in NIM, the MiMPCs and MSCs were cultured in a basal medium (DMEM-F12, 5% FBS, insulin-transferrin-selenium-X [ITS-X], penicillin-streptomycin [PS]; all reagents obtained from ThermoFisher) for 48 hours, at which point the medium samples were collected, filtered, and designated as 48-hour basal conditioned medium (48 hours BCM) for use in functional bioassay DRG culture experiments (see below).

Immunofluorescence Labeling

The culture medium was aspirated from the MiMPC, MSC, and Schwann cell control cultures (cell line sFN92.6, obtained from ATCC, Manassas, VA), and cells were washed with phosphate buffered saline (ThermoFisher). Cells were fixed with 4% paraformaldehyde (Electron Microscopy Sciences, Hatfield, PA) for 20 minutes, washed, and treated for 1 hour with hot 10 mm sodium citrate (Sigma-Aldrich) in 10% ethanol for antigen retrieval. After blocking with 5% FBS for at least 1 hour at room temperature, the cultures were incubated with primary antibodies for at least 4 hours at room temperature, or overnight at 4°C. Immunofluorescence was carried out to localize the following cell markers on MiMPC, MSC, and Schwann cell cultures both before and after neurotrophic induction treatment: Schwann markers—glial fibrillary acidic protein (GFAP) (chicken IgY; cat. ab4674), P75/NGFR (rabbit IgG; cat. ab8874), S100B (rabbit monoclonal IgG; cat. ab52642); pluripotency markers—Sox2 (rabbit IgG; cat. ab97959), SSEA4 (mouse IgG; cat. 560307), and Oct3/4 (mouse IgG; cat. 560308); and MSC markers—CD44 (mouse monoclonal IgG; cat. MAB7045), CD73 (mouse monoclonal IgG; cat. ab81720), and CD105 (goat IgG; cat. AF1097). Primary antibodies were diluted in block buffer per manufacturer's instructions. Samples were incubated with secondary antibodies, diluted in block buffer per manufacturer's instructions, for 1 hour at room temperature. All cells were nuclear-counterstained with 4′,6-diamidino-2-phenylindole dihydrochloride (DAPI; ThermoFisher) for approximately 1 minute. SSEA4 and Oct3/4 antibodies were obtained from BD Biosciences (Franklin Lakes, NJ). CD44 and CD105 antibodies were obtained from R&D Systems. All other antibodies were purchased from abcam (Cambridge, MA). Secondary antibodies used were Alexa-Fluor 488 conjugates from ThermoFisher (rabbit anti-goat IgG

[cat. A27012], goat anti-mouse IgG [A10680], goat anti-chicken IgY [A11039], donkey anti-rabbit IgG [A21206]).

ELISA

Neurotrophic induction was performed on MiMPC cultures as described above. After induction treatment, conditioned media were collected from the cultures and concentrations of brain-derived neurotrophic factor (BDNF), ciliary NTFs (CNTF), glial cell-derived neurotrophic factor, (GDNF), neurotrophin-3 (NT-3), and nerve growth factor (NGF) were assayed via DuoSet ELISA kits (R&D Systems) according to the manufacturer's protocols.

Additional ELISAs for non-neurotrophins were also performed on conditioned media, including interleukin-6 (IL-6), leukemia inhibitory factor (LIF), tumor growth factor-β (TGF-β), interleukin-10, neuregulin (NRG), and fibroblast growth factor 9 (DuoSet ELISA kits from R&D Systems).

Gene Expression Assay

RNA was isolated from induced MiMPCs using RNeasy Plus Mini Kit (Qiagen, Valencia, CA) according to manufacturer's protocol. cDNA was synthesized using Invitrogen's SuperScript III First-Strand kit (ThermoFisher). Real-time polymerase chain reaction (RT-PCR) was performed using SYBR Green PCR Master Mix from Life Technologies (ThermoFisher) and a StepOnePlus Real Time PCR machine (Thermo-Fisher). All gene expression levels were normalized to that of 18S rRNA as the control housekeeping gene. Primers for BDNF, GDNF, CNTF, and 18S rRNA were obtained from Qiagen, and the primer for NGF was obtained from Integrated DNA Technologies (Coralville, IA).

RT^2 Profiler PCR Arrays (Qiagen) were used to assay for expression of human neurotrophins and receptors, and inflammatory cytokines and receptors. Arrays were run using RT^2 SYBR Green ROX qPCR Mastermix (Qiagen) as per manufacturer's protocols. PCR data analysis and heat map generation were done via Qiagen's online RT^2 Profiler PCR Array Data Analysis (version 3.5; http://pcrdataanalysis.sabiosciences.com/pcr/arrayanalysis.php).

Dorsal Root Ganglia /MiMPC Coculture Assay

DRGs were harvested from day 9 chick embryos, using a previously described protocol [7]. The isolated DRGs were plated one per well of a 12-well plate coated with poly-D-lysine and laminin (both supplied by Sigma-Aldrich). Poly-D-lysine solution (100 ng/ml) was prepared and dispensed into each well of a 12-well plate, allowed to coat the plate for 3 days at 4°C with gentle rocking. Laminin (10 μg/ml) was prepared and applied as a supplemental coating in the same manner as poly-D-lysine.

The DRGs were allowed to adhere to the substrate in medium consisting of DMEM-F12 and 5% FBS, further supplemented with 10 ng/ml each of basic FGF-2, epithelial growth factor (EGF), and NGF. After a 3-day settlement period, medium on DRGs was exchanged for 48-hour basal conditioned medium (48-hour BCM) collected from: (a) NI-MiMPCs, (b) GM-MiMPCs, (c) NI-MSCs, or (d) GM-MSCs. Control DRGs were cultured in cell-free unconditioned basal medium consisting of DMEM-F12, 5% FBS, ITS-X, and pen-strep. All DRGs were cultured for 5 days. Cultures were then immunostained as outlined previously. Briefly, DRGs were fixed with 4% paraformaldehyde, incubated in hot sodium citrate for antigen retrieval, blocked in 5% FBS and incubated with chicken IgY anti-heavy neurofilament primary antibody (abcam; cat. ab4680) diluted to 1:10,000 overnight at 4°C. AlexaFluor 488 conjugated secondary antibody (ThermoFisher; cat. A11039) was allowed to incubate for 1 hour at room temperature at a 1:300

dilution with blocking buffer. Neurite outgrowth was quantitatively assessed (see below).

Trk Signaling Inhibition

To assess the involvement of Trk receptor-mediated neurotrophin signaling, the Pan-Trk inhibitor, GNF-5837 (Sigma-Aldrich), was used at a concentration of 24 nM, which exceeded IC$_{50}$ values (7–11 nM for TrkA, TrkB, and TrkC) reported in the literature [8]. GNF-5837 was supplemented to 48-hours BCM from neurotrophically induced MiMPCs (NI-MiMPCs) and control MiMPCs (GM-MiMPCs), and neurotrophically induced MSCs (NI-MSCs) and control MSCs (GM-MSCs), which were subsequently used to culture chick DRGs for 5 days. Cultures were paraformaldehyde-fixed and immunostained for heavy neurofilament, and branching complexity of neurite outgrowth was assessed (see below).

JAK/STAT3 Inhibition

To assess the involvement of JAK/STAT3-mediated signaling, cucurbitacin I (Sigma-Aldrich), a selective inhibitor of the JAK/STAT3 signaling pathway that suppresses the levels of tyrosine phosphorylated STAT3 [9], was used at a concentration of 60 nM. Cucurbitacin was supplemented to 48-hours BCM from NI-MiMPCs and control MiMPCs, and NI-MSCs and control MSCs, which were subsequently used to culture chick DRGs for 5 days. Cultures were paraformaldehyde-fixed and immunostained for heavy neurofilament, and branching complexity of neurite outgrowth was assessed (see below).

Immunofluorescence Staining of DRG

DRG cultures were fixed in buffered 4% paraformaldehyde and permeabilized for antigen retrieval with hot 10 mM sodium citrate for 1 hour, blocked with 5% FBS, and incubated with mouse anti-human heavy neurofilament (1:500; abcam) in block buffer overnight at 4°C. After rinsing, cultures were then incubated with fluorescently labeled secondary antibodies (1:300; AlexaFluor 488 goat IgY [cat. A11039]; Invitrogen, Carlsbad, CA) for 1 hour at room temperature.

Quantitation of Neurite Extension

Fluorescent DRG image tiles were processed with MetaMorph (Molecular Devices, Sunnyvale, CA), and digitally stitched together using open source software Fiji/NIH ImageJ [10]. All grayscale images were thresholded to create binary bitmap images. Neurite extension densities were measured using the Sholl analysis plugin function within Fiji. The algorithm automatically retrieves data from two-dimensional (2D) or three-dimensional (3D) images to perform a regression analysis and generate the metrics for Sholl-based dendrite arborization [11]. All images were taken at ×4 magnification using an inverted microscope (Olympus IX81) with a motorized stage controlled through MetaMorph, and the scale used was 620 px = 1 mm.

Neurite extension lengths were quantified based on images of DRGs cultured on 2D aligned nanofibrous poly-ε-caprolactone (PCL) scaffolds prepared by electrospinning (see below). All images for scaffold cultures were taken at ×10 using the inverted Olympus scope (IX81). Tracings were converted from pixel length into μm measurements using the scale of 1245 px = 800 μm.

Preparation and Photocrosslinking of Methacrylated Gelatin (mGelatin)

mGelatin was prepared by reacting gelatin (type B) (Sigma-Aldrich) with methacrylic anhydride using our recently published

protocol [12]. Photocrosslinking was initiated using the visible-light sensitive initiator lithium phenyl-2,4,6-trimethylbenzoylphosphinate (LAP) [13].

Fabrication of Electrospun Scaffolds

A PCL-mGelatin composite scaffold was prepared using a modification of our recently published procedure [14]. Two separate solutions were prepared: (a) 14.0% wt/vol PCL (80 kDa; Sigma-Aldrich) in 2,2,2-trifluoroethanol (Sigma-Aldrich); and (b) 18% methacrylated-gelatin (mGelatin) in 95% 2,2,2-trifluorethanol in water to generate a mGelatin:PCL (40:60) composite nanofibrous scaffold. Two 10-ml syringes were separately filled with the PCL and mGelatin electrospinning solution, and they were fitted with a stainless steel 22G blunt-ended needle that served as a charged spinneret, and directed at a single central rotating mandrel (surface velocity of 10 m/s) in a custom-designed electrospinning apparatus. The speed of the mandrel was sufficiently fast to align the collected fibers in a single direction. A flow rate of 2 ml/hour was maintained with a syringe pump (Harvard Apparatus, Holliston, MA). A power supply (Gamma High Voltage Research, Inc., Ormond Beach, FL) applied a +15–20 kV potential difference between the needles and grounded mandrel to obtain a Taylor cone for mGelatin and a +7–10 kV potential difference for PCL. Additionally, two aluminum shields charged to +5kV were placed perpendicular to and on either side of the mandrel to better direct the electrospun fibers toward the grounded mandrel. The distance between the mandrel and the needle was 15 cm for mGelatin fibers and 15 cm for the PCL fibers. The composite electrospun scaffold was generated to a final thickness of 100 μm. The procedure was the same for creating randomly aligned scaffolds, except that the mandrel surface velocity was 0.75 m/s.

Preparation of Aligned Scaffolds and Seeding of DRGs

A 8% wt/vol mGelatin solution in HBSS (480 mg in 6 ml) was prepared, to which 1.8 mg of photoinitiator LAP was added to achieve a 0.3% wt/vol concentration of the photoinitiator. A 3.0 × 5.5 cm sheet of composite scaffold consisting of either aligned or random fibers prepared as described above was wetted with 540 μl of the mGelatin solution. Following this, each scaffold was folded lengthwise (along the 5.5 cm side) into thirds. The remaining 60 μl of the mGelatin solution was then evenly applied on top of the folded random scaffold, on top of which the folded aligned scaffold was placed. The six-layered construct was then exposed to visible light for 3 minutes (1.5 minutes on each side) to photopolymerize the construct. After construction of the completed multilayer scaffold, five cylinders of 8 mm diameter were punched out with a punch biopsy.

All scaffolds were prepared on the same day as DRG isolations and kept in basal medium (DMEM-F12, 5% FBS, ITS-X, and penstrep) until needed. DRGs were seeded as follows: (a) upon isolation from the chick embryo, DRGs were individually pipetted, and pipette tips were held above the scaffold and below the level of medium in the well; and (b) to ensure more accurate placement on the scaffolds, DRGs were allowed to descend out of the pipette via gravity, rather than being actively pipetted.

Statistical Analysis

All data were expressed as mean ± standard deviation. Statistical analysis was performed using one-way analysis of variance (ANOVA) followed by Games-Howell post hoc testing for all experiments except DRG neurite extensions, where Tukey's HSD post hoc was used. A threshold of $p < .05$ was used to determine statistical significance.

## iPSCs Can Be Differentiated into Cells with Neural Cell Phenotype

The iPSCs used in this study were obtained by lentiviral reprogramming of adult human bone marrow MSCs as described previously [6]. Morphological examination and immunofluorescence staining confirmed that these cells grew in colonies of small, undifferentiated cells, and that through their usage and numerous passages, they retained expression of pluripotency markers SSEA4, Oct3/4, and Sox2 (Fig. 1A–1D).

Feeder-free iPSCs were subsequently grown to confluency and differentiated into mesenchymal-lineage MiMPCs. On the third day of the differentiation period, a group of MiMPCs were set aside, paraformaldehyde-fixed and stained for mesenchymal, Schwann, and pluripotency markers in order to chart their transition. On day 3, it was shown that MiMPCs expressed mesenchymal markers CD44 and CD105, but was only weakly positive for CD73. MiMPCs were positive for all Schwann cell markers, and were positive for Sox2, faintly positive for Oct3/4, and negative for SSEA4 (Fig. 1E). This prompted us to extend the differentiation period in the protocol out to 7 days total, in order to give the cells more time to fully differentiate into a mesenchymal-like cell. With a 7-day differentiation protocol, cells were strongly positive for all mesenchymal markers, and negative for all pluripotency markers (Fig. 2).

These cells have been shown to be a distinct population of cells that express mesenchymal cell markers, such as CD44, CD73 and CD105, and are capable of behaving similarly to MSCs in that they can be differentiated along osteogenic, as well as adipogenic and chondrogenic lineages [6]. Phase contrast microscopy showed morphological changes examined indicating that while feeder-free iPSCs grew in undifferentiated colonies (Fig. 1A), after differentiation, MiMPCs (Fig. 1B) were morphologically similar to control MSCs (Fig. 1C). Immunohistochemistry also showed that MiMPCs, like MSCs and Schwann cell controls, expressed mesenchymal markers (CD44, CD105, and CD73) and neurologically relevant cell markers (GFAP, S100B, and p75-NGFR), the expression of which was not affected upon neuroinductive treatment (NI-MiMPCs and NI-MSCs). Similarly, noninduced MiMPCs and MSCs grown in growth medium (GM-MiMPCs and GM-MSCs) were also positive for mesenchymal and Schwann cell markers (Fig. 2).

MiMPCs and MSCs Maintain p75/NGFR and GFAP Expression

MSCs and MiMPCs expressed glial fibrillary acidic protein (GFAP) and low affinity p75 NGF receptor (p75/NGFR) both before and after neuroinductive (NI) treatment (Fig. 2). GFAP is an intermediate filament and is a major component of the astrocyte cytoskeleton, and may also play a role in maintenance of myelination [15]. p75/NGFR is important for axonal growth and Schwann cell migration during development, with severe peripheral neuronal defects resulting from its absence [16]. Presence of these neural markers suggested that both MSCs and MiMPCs phenotypically resembled Schwann cells regardless of whether or not the cells were treated with NI medium.
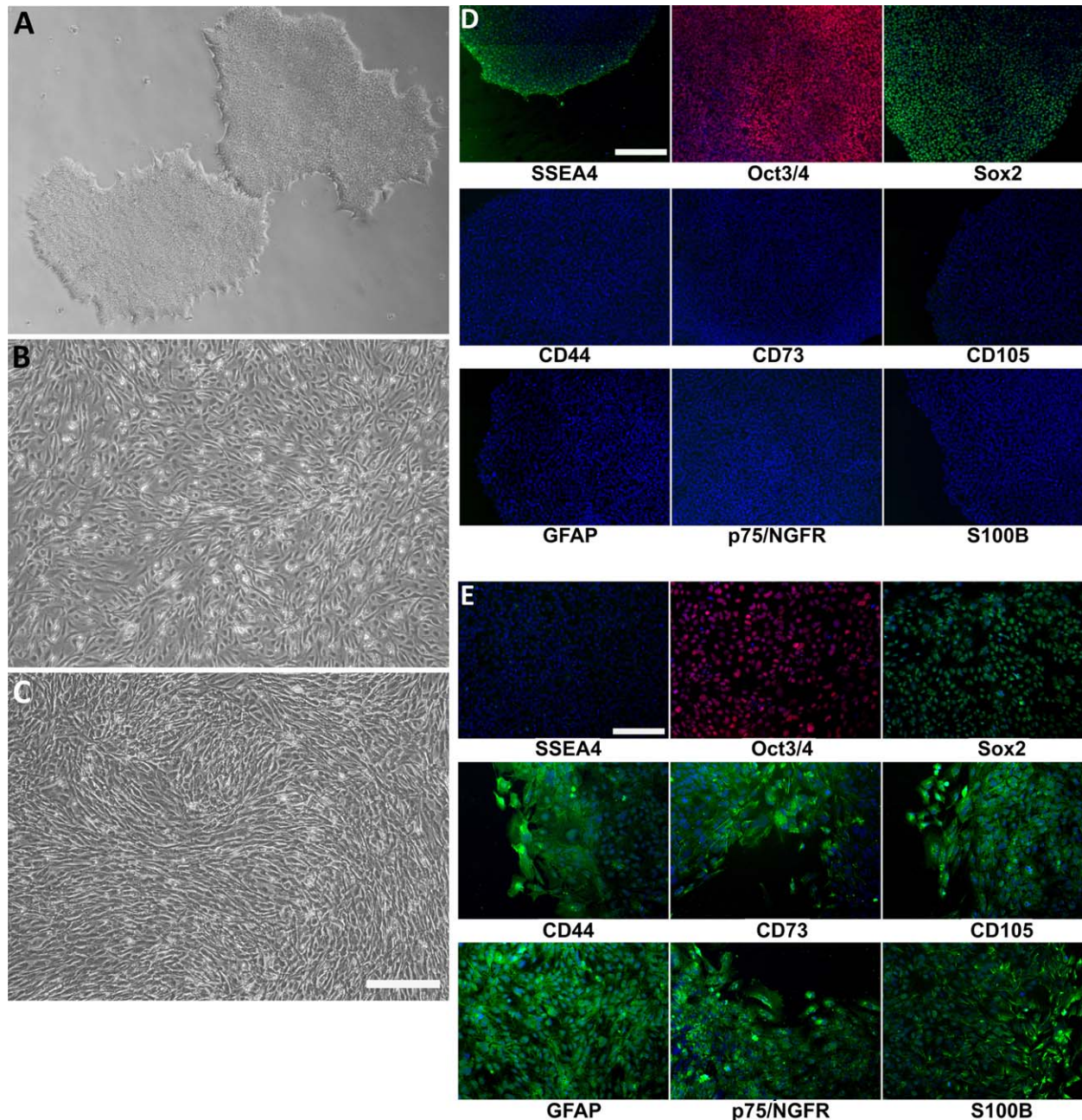
Figure 1. Morphology of induced mesenchymal progenitor cells (MiMPCs) and mesenchymal stem cells (MSCs) examined by phase contrast microscopy. **(A):** Undifferentiated colonies of human induced pluripotent stem cells (iPSCs) reprogrammed from human bone marrow MSCs [6]. Cells grew to confluent colonies on Matrigel, in feeder-free culture. **(B):** Confluent MiMPC cultures differentiated from iPSCs. All MiMPC cultures resembled MSCs in morphology, with no remaining iPSC morphology. **(C):** Confluent control MSCs isolated from human bone marrow (passage 5). Each cell type ($n > 5$) was cultured over the course of all experiments performed in this study. Cells in (A–C) were imaged at $\times 4$ magnification (Bar $= 560$ μm.) **(D, E):** MiMPCs were fixed and immunofluorescently stained on the third day of differentiation; colonies of confluent iPSCs served as controls. Cells were stained for MSC markers (CD44, CD73, and CD105), Schwann cell markers (GFAP, p75/NGFR, and S100B), and pluripotency stem cells markers (Sox2, SSEA4, and Oct3/4). All cells were counterstained with 4′,6-diamidino-2-phenylindole dihydrochloride. (D) iPSCs were negative for MSC and Schwann cell markers, but stained positively for pluripotency markers, indicating the maintenance of stemness throughout culture and passaging. (E) MiMPCs cells were strongly positive for CD44 and CD105, and weakly positive for CD73. MiMPCs also stained positive for all Schwann cell markers, positive for Sox2, weakly positive for Oct3/4, and negative for SSEA4, showing their transition and demonstrating the need for long differentiation period. Cells in (D, E) were imaged at $\times 10$ magnification (Bar $= 220$ μm). Abbreviation: GFAP, glial fibrillary acidic protein.

MiMPCs Produce BDNF as Well as Other Non-Neurotrophic Factors After Neurotrophic Induction

Analysis of gene expression using PCR array panels for neurotrophins and inflammatory cytokines showed an upregulation in genes relevant to nerve regeneration, including IL-6, LIF, IL-1B, and osteopontin (SPP1) in NI-MiMPCs, compared with GM-MiMPCs and to MSC groups (Supporting Information Fig. 1). ELISA results confirmed that the upregulated genes correlated with increased,
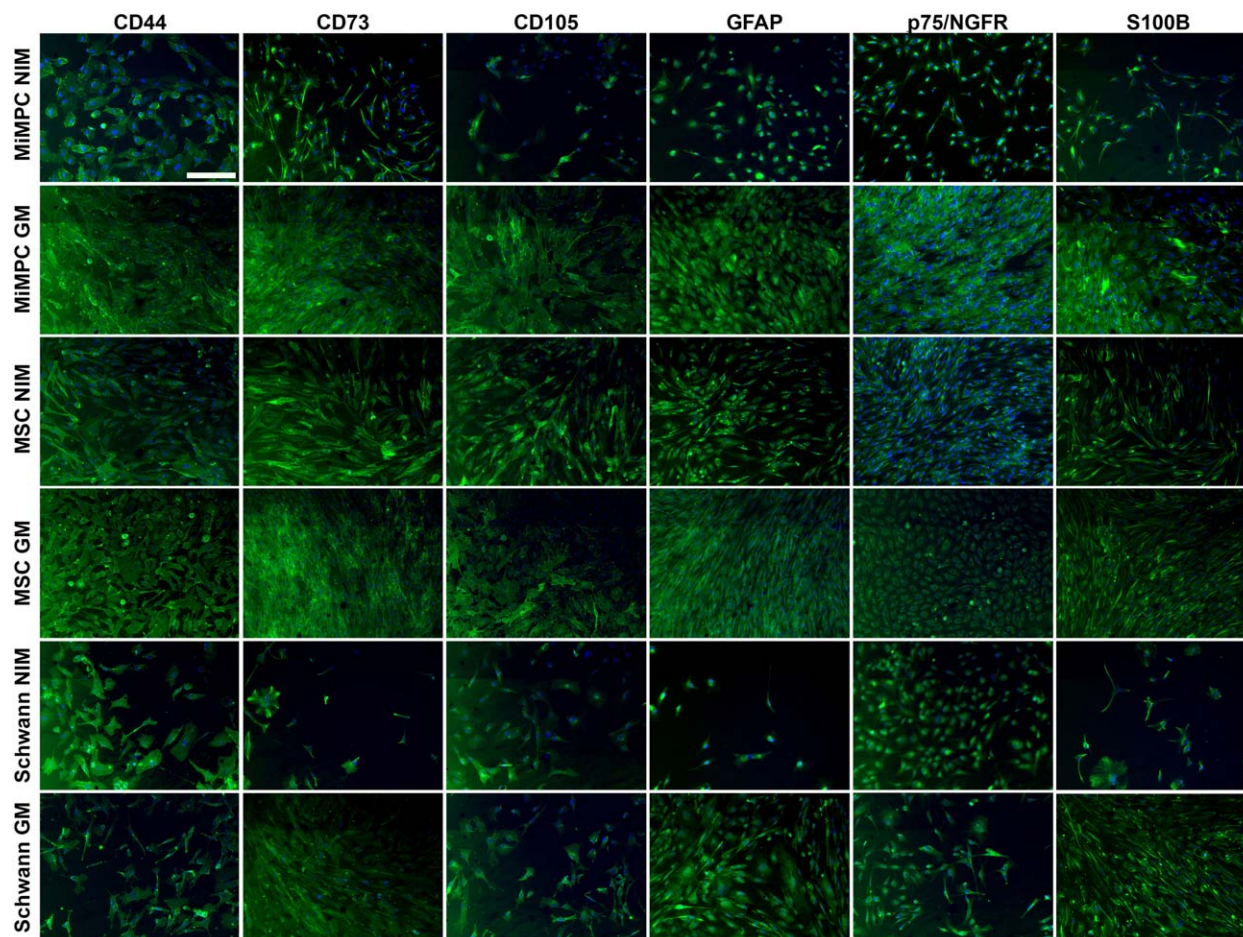
Figure 2. Expression of neurological and mesenchymal cell markers in MiMPCs and MSCs during neurotrophic induction examined by immuno-fluorescence. MiMPCs and MSCs were cultured in NIM or growth medium (GM). Neurotrophically induced MiMPCs and MSCs were fixed and stained with antibodies against MSC markers (CD44, CD73, CD105) and Schwann cell markers (GFAP, p75/NGFR, and S100B). Neurotrophically induced and noninduced MiMPC and MSC cultures stained positive for all MSC and Schwann cell markers. Schwann cells were stained as a control, and were positive for all markers. All cells were counterstained with 4′,6-diamidino-2-phenylindole dihydrochloride. All images were taken at ×10 magnification and are representative of all fields. Bar = 220 μm, $n = 2$. Abbreviations: GFAP, glial fibrillary acidic protein; GM, growth medium; MiMPCs, induced mesenchymal progenitor cells; MSCs, mesenchymal stem cells; NIM, neurotrophic induction medium.

corresponding protein levels in cell culture supernatant. We did not conduct an ELISA to detect IL-1B, as 10 ng/ml of IL-1β was included in the NI medium.

As there was only approximately a 40% correlation between mRNA upregulation and protein production [17–19], we performed ELISAs to confirm the production of each of the aforementioned factors. Our ELISA data show that under normal growth medium conditions, control MSCs produced low levels of BDNF. Following neurotrophic induction, NI-MSCs produced significantly higher levels of BDNF. Although MiMPCs exhibited many of the same characteristics seen in MSCs, our results showed that GM-MiMPCs were able to produce small amounts of BDNF; in fact, BDNF production levels from GM-MiMPCs were comparable to those seen from induced MSCs. However, our ELISAs detected significantly higher BDNF production from MiMPCs after treatment with NI medium (Fig. 3).

BDNF production by MiMPCs was further enhanced when 10 ng/ml IL-1β was added to the NI medium. Conditioned medium assayed by ELISA during and after the induction period showed a consistent increase in BDNF concentrations compared with both

normal NI medium and growth controls. The most marked increase in BDNF production by MiMPCs when IL-1β was present occurred at day 7, with an approximately fivefold increase in BDNF levels compared with that in MiMPCs cultured in NI-medium without IL-1β. Although this enhanced production of BDNF tapered off after the inductive medium was removed, conditioned medium collected 48-hours after induction still showed a twofold increase in BDNF concentration. While MSCs also showed a significant increase in BDNF production at Day 7, the total concentration was well below the levels detected in the MiMPC conditioned medium. The significant increase in BDNF production did not persist in conditioned medium taken from either MiMPCs or MSCs 48 hours after induction. However, at this time point, BDNF concentration from MiMPCs induced with NI-medium supplemented with IL-1B still remained higher than MiMPCs induced with normal NI-medium (Fig. 3). For this reason, we continued supplementing our NI-medium with 10 ng/ml IL-1β.

Other cytokines have been shown previously to improve nerve regeneration after injury, among them IL-6 [20, 21], LIF [22, 23], osteopontin, clusterin [24], and osteonectin [25–27].
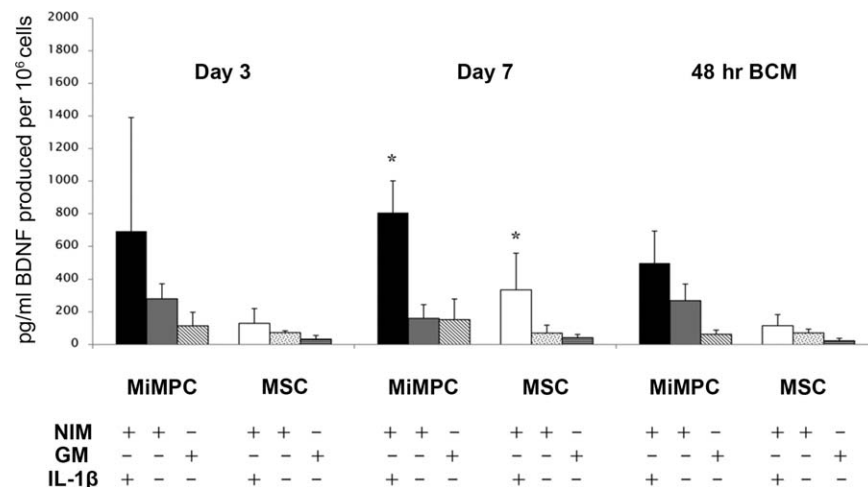
Figure 3. Effect of IL-1β on BDNF production in MiMPCs and MSCs. MiMPCs and MSCs were cultured in NIM, GM, or NIM including 10 ng/ml interleukin-1β (IL-1β). The presence (+) or absence (−) of NIM, GM, and/or IL-1β is as indicated. BDNF ELISA results showed that the presence of IL-1β in NIM significantly enhanced BDNF production by MiMPCs, particularly on day 7 (∼5-fold increase). This effect was less pronounced at 48-hours post-induction, although the level of BDNF in MiMPCs induced with NIM + IL-1β was still ∼2-fold higher than in NIM alone. *, $p < .05$ compared with GM controls, $n > 3$. Abbreviations: 48-hours BCM, 48-hour basal conditioned medium; BDNF, brain-derived neurotrophic factor; ELISA, enzyme-linked immunosorbent assay; NIM, neurotrophic induction medium; GM, growth medium; IL-1β, interleukin-1β; MiMPCs, induced mesenchymal progenitor cells; MSCs, mesenchymal stem cells.

Interestingly, the cytokine ELISA results on medium samples conditioned by NI-MiMPCs and NI-MSCs also demonstrated marked increases in the concentration of these factors (Fig. 4).

We assayed conditioned medium collected at days 3 and 7 of the NI medium treatment, as well as basal medium conditioned for 48-hours after the NI treatment period was over. The ELISA data in Figure 4 show that BDNF, IL-6, and osteonectin production remained relatively constant throughout and after the induction period (Fig. 4A, 4C, 4E), but there was a significant decrease in osteopontin and LIF production during and after the NI treatment period (Fig. 4B, 4D). Since osteopontin and LIF concentration levels were low in the NI-MiMPC conditioned basal medium, we focused on BDNF, IL-6, and osteonectin for our next set of experiments on the effects of MiMPCs and MSCs of neurite extension in DRG cultures.

Neurotrophically Induced MiMPCs Enhance Dorsal Root Ganglia Neurite Extension Complexity

We evaluated the effect of neurotrophically induced cells on nerve growth by culturing DRGs with conditioned medium from NI-MiMPCs and NI-MSCs (Fig. 5). All DRGs were dissected from 9-day-old chick embryos.

DRG neurite extension complexity was evaluated by Sholl analysis [28] using ImageJ. A morphological examination of immunofluorescence staining showed that DRGs cultured with both conditioned medium from NI- and GM-MiMPCs appeared to have significantly improved neurite outgrowth, compared with either control cultures or those cultured with conditioned media from NI-MSCs. DRGs cultured in conditioned medium from GM-MSCs also exhibited significantly enhanced neurite outgrowth. This demonstrated that MSCs and MiMPCs, particularly the latter, were producing factors that enhanced nerve growth.

Our first objective was to determine if BDNF production by these cells played a role in this improvement. The involvement of BDNF was tested by examining the effect of inhibiting the action of the neurotrophin Trk-receptor on DRG neurite outgrowth. The pan-Trk receptor inhibitor drug, GNF5837 (24 nM), was co-

administered to the MiMPC conditioned medium treated DRGs. As shown in Figure 5A, DRG growth appeared to be only slightly reduced in complexity and size. The Sholl analysis results showed that, upon GNF5837 cotreatment, all conditioned medium treated groups, except for medium collected from NI-MiMPCs, experienced a marked decrease in neurite extension density such that they were no longer significantly different from controls, with average number of intersections decreasing from 319 to 139 [GM-MiMPC], 313 to 170 [GM-MSC], and increasing minimally from 173 to 215 [NI-MSC], as opposed to only a 10% decrease in measured branching density in cultures containing NI-MiMPC conditioned medium (286–257) (Fig. 5B). Furthermore, as our cells did not produce detectable levels of the neurotrophins, NGF, NT-3, CNTF, or GDNF, with the latter two not acting through the Trk receptors, this observation suggested that additional non-NTFs were likely being produced by NI-MiMPCs that were capable of initiating neurite extensions, acting independently of the Trk-receptors.

As many published investigations have suggested a role for IL-6 in nerve regeneration [20, 21, 29], and as our results suggested that BDNF was unlikely to be the only factor involved in enhancing neurite extension density, we sought to block the effects of IL-6 to determine if neurite density would be affected. As IL-6 signals through the Jak/STAT pathway, we targeted the inhibition of this pathway with a pharmacological blocker, cucurbitacin-I [9]. Results from the Sholl analysis showed that treatment with cucurbitacin-I decreased neurite complexity to the extent that the effects of the conditioned medium from noninduced cells was no longer significantly different from that seen in control cultures, with average numbers of intersections decreasing from 319 to 274 (GM-MiMPC), and 313 to 241 (GM-MSC). Although the average number of intersections increased slightly upon the addition of cucurbitacin-I in the NI-MiMPCs (286–425) and NI-MSCs (173–230) groups, the extent of standard deviation prevented the data from achieving statistical significance. However, conditioned medium from NI-MSCs still enhanced complexity of DRG neurite extensions compared with controls (Fig. 5B). The more pronounced effect of
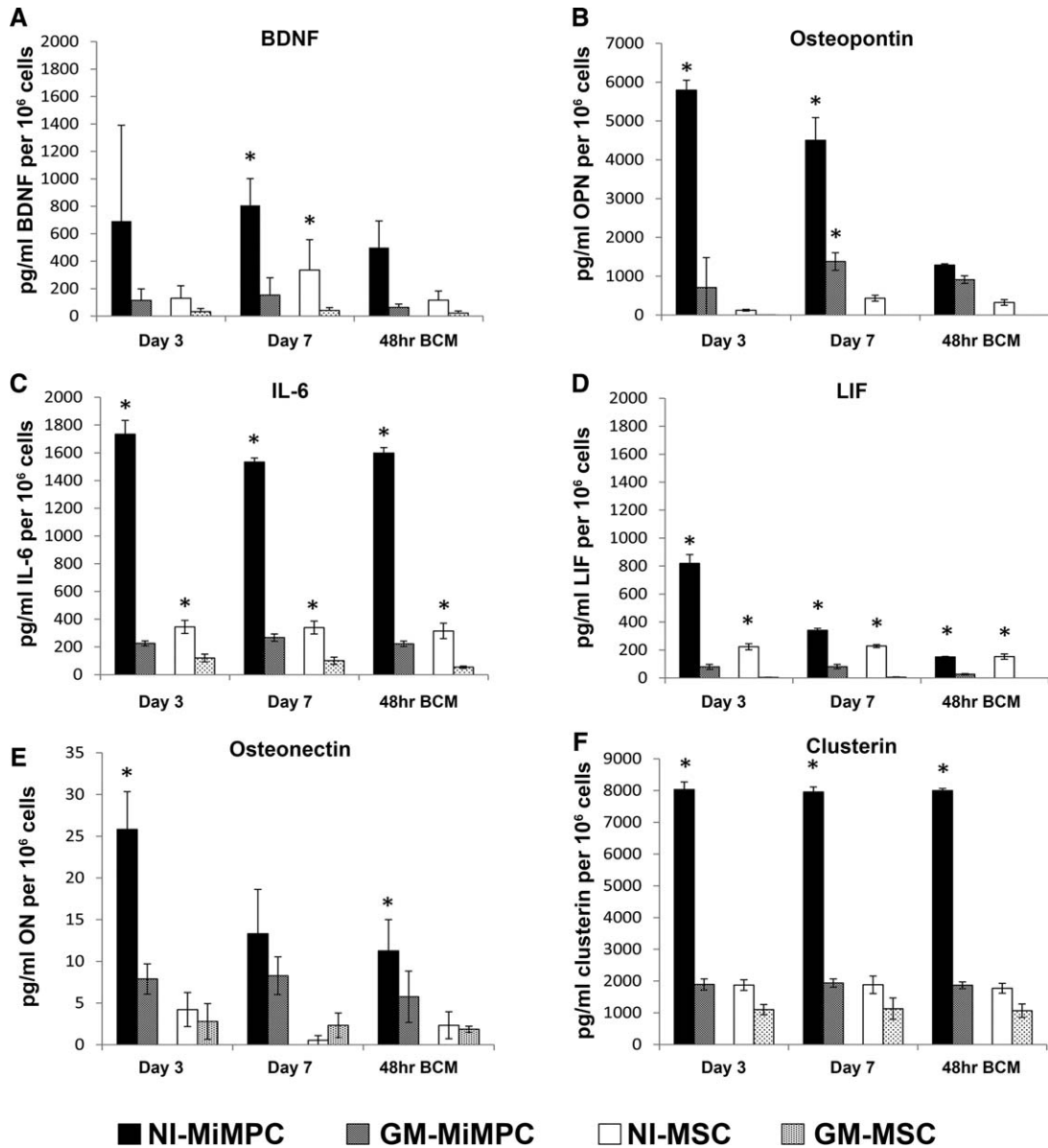
Figure 4. Production of neurotrophic factors by NI-MiMPCs and MSCs, quantified via ELISA. MiMPCs and MSCs were cultured in neurotrophic induction medium or growth medium. Conditioned media taken from days 3 and 7 of induction culture, and basal conditioned medium taken from cultures 48 hours post-induction (48-hour BCM). The conditioned media assayed include those from MiMPCs (induced, NI-MiMPCs; uninduced, GM-MiMPCs), and from MSCs (induced, MI-MSCs; uninduced, GM-MSCs), as well as basal medium (controls). Medium was assayed for levels of **(A)** BDNF, **(B)** Osteopontin, **(C)** IL-6, **(D)** LIF, **(E)** osteonectin, and **(F)** clusterin. All ELISA results are expressed in pg/ml or ng/ml produced per million cells. Medium taken from NI-MiMPC cultures contained high levels of all assayed factors compared with GM-MiMPCs, NI-MSCs, and GM-MSCs. BDNF, IL-6, osteonectin, and clusterin exhibited relatively constant secretion levels, while osteopontin and LIF showed decreased expression levels during induction treatment and the 48-hour post-induction period. *, $p < .05$, compared with GM controls, $n \geq 3$ for all assays. Abbreviations: BDNF, brain-derived neurotrophic factor; ELISA, enzyme-linked immunosorbent assay; IL-6, interleukin-6; LIF, leukemia inhibitory factor; MSCs, mesenchymal stem cells; NI-MiMPCs, neurotrophically induced-MiMPCs.

the addition of cucurbitacin-I to the DRG cultures, however, was the decrease in extension length (see below).

Neurotrophically Induced MiMPCs Enhance Dorsal Root Ganglia Neurite Extension Lengths

We next determined the influence of NI-MiMPCs on DRG neurite length. This was carried out using embryonic chicken DRGs cultured on electrospun 2D aligned nanofibrous PCL/gelatin scaffolds, which afforded more consistent and reliable measurements of neurite length (Fig. 6), as the aligned fibers helped to better

organize neurite outgrowth, and allowed visualization and more precise measurements of axonal distance covered.

In doing so, we found that culturing DRGs in conditioned medium from any cell group significantly increased the length of neurite extensions compared with controls, although there was no difference between conditioned medium taken from any cell group (maximum length achieved with conditioned medium was 2,650 μm, while control lengths averaged 1,389 μm, an increase of 47.6%). There was no difference in lengths measured between induced and noninduced cells, or MiMPC and MSC groups (Fig. 6B).

Again, we co-administered 24 nM of GNF5837 to determine if any factor acting through the Trk receptors played a role in altering length of the extensions. It has been reported that BDNF, acting through TrkB, is capable of activating STAT3, which is essential in axon extension [30, 31]. However, the addition of the pharmacological blocker did not result in a difference in neurite extension lengths (Fig. 6B). This led us to conclude that, as with neurite initiation, BDNF was unlikely to be the sole factor produced by the NI- or GM-MiMPCs that contributed to neurite extension length, suggesting the action of other signaling pathway(s).

IL-6 Produced by MiMPCs Contribute to DRG Neurite Extension Length

Our results showed that GNF5837 inhibition of the Trk receptors did not affect the enhancement of neurite extension length by MiMPCs, as there was no observable or measurable difference in lengths between cultures where GNF5837 was absent or present (Fig. 6B). In view of the apparent difference in neurite extension density between exposure to NI-MiMPCs and GM-MiMPCs in the presence of the Trk-receptor inhibitor, we postulated that the induced MiMPCs must produce some factors, besides BDNF, to drive increased neurite extension density through non-Trk receptor mediated signaling, particularly the Jak/STAT pathway. Therefore, we looked to the presence of other secreted non-neurotrophin factors. Our PCR and ELISA data confirmed that NI-MiMPCs produced and maintained a high level of IL-6 compared with uninduced cells (see Supporting Information Figs. 1, 4), so our next set of experiments focused on the possible involvement of IL-6 on neuritogenesis and neurite extension length.

Cytokines in the IL-6 cytokine superfamily signal through the gp130 receptor to activate the Jak/STAT3 pathway, which has been shown to be important in the growth of neurite extensions and nerve regeneration [32, 33]. Our ELISA results (Fig. 4) showed that NI-MiMPCs were able of producing some cytokines in this family, including IL-6 and LIF, but not others, such as oncostatin-M and ciliary NTFs (CNTF) (data not shown). We postulated that these pro-inflammatory cytokines secreted into the conditioned medium from NI-MiMPCs could act through the Jak/STAT3 pathway to maintain improved neurite outgrowth, even when Trk-receptors were blocked.

To test this possibility, we chose the drug cucurbitacin-I to inhibit the Jak/STAT3 pathway [9]. Upon administration of cucurbitacin-I (60 nM) to the conditioned media, a dramatic decrease in neurite extension length and size of DRG cultures was observed (Fig. 6A). DRGs treated with cucurbitacin-I appeared to have stunted extension length while maintaining comparable number of neurite extensions. Sholl analysis confirmed that neuritogenesis, and therefore, density of neurite extensions, appeared unaffected (Fig. 6B). This indicated that while the actions of the Jak/STAT3 pathway and, by implication, the action of IL-6, was critical to neurite length, it did not play a crucial role in neuritogenesis.

To better measure neurite extension lengths in the presence of a Jak/STAT3 pharmacological inhibitor, DRGs were cultured on 2D nanofiber scaffolds, and treated with conditioned media containing 60 nM of cucurbitacin-I. We found that these DRG cultures on 2D nanofibrous scaffolds did not produce neurite extensions at all when grown in the presence of cucurbitacin-I, contrary to what was observed in cultures maintained on tissue culture plastic. Physical topography of cell culture substrate surfaces is well known to influence cell growth [34–36]. Our observations suggested that cucurbitacin-I could have affected the ability of the outgrowing neurites in interacting with different substrate surfaces, that is, tissue culture plastic versus nanofibers. Since there were no observable extensions from the cucurbitacin-I treated group, these measurements were not included in Figure 6B. As the complex, aligned topography is likely to be more relevant to tissue architecture in vivo, these results are consistent with an important role of IL-6 signaling through the Jak/STAT pathway in mediating the improvement of the length and complexity of neurite extensions by the MSC/MiMPC conditioned media.

DISCUSSION

In this study, we have shown that MiMPCs are capable of supporting and enhancing neuritogenesis and axon length in DRG cultures. Their neurotrophic effects are similar to those of MSCs, and are enhanced with NI-medium treatment, although the latter exhibit effective neurotrophic support even without NI-medium treatment.

The goal of this study was to determine if NI-MiMPCs, which are generated from iPSCs and are thus available without additional, invasive cell harvesting, are capable of providing the support necessary for nerve regeneration. Our ultimate objective is to identify a candidate therapeutic cell type to support nerve growth akin to that seen by Schwann cells or induced MSCs. Our results suggest that MiMPCs may indeed be applicable for cell therapy for nerve injuries as nerve outgrowth in the DRG is enhanced by treatment with conditioned medium taken from MiMPC cultures.

MiMPCs generated from iPSCs morphologically resemble typical MSCs, and differ substantially from the parent iPSCs. iPSC colonies are negative for all mesenchymal and Schwann cell markers, but are instead positive for the pluripotency markers, SSEA4, Sox2, and Oct3/4. Our previous study demonstrated the pluripotency nature of the bone marrow MSC-derived iPSC line used here [6]. In contrast, characterization of MiMPCs showed positive staining for many of the same cell surface markers as both MSCs and Schwann cells, including CD44, CD73, CD105, GFAP, S100B, and P75/NGFR.

It is noteworthy that MiMPCs show expression of p75/NGFR. A study by Bentley and Lee [16] showed that the lack of p75/NGFR was linked to a deficit in Schwann cell migration and coverage, as well as a substantial reduction in nerve bundle and axon formation. Interestingly, there have also been reports stating the negative effects of p75 after injury, and that it may have a role in axon apoptosis and death signaling pathways [37, 38]. However, the literature related to p75 is insufficient to confirm whether or not the presence of p75 is helpful or harmful in terms of axon regeneration after injury, though some data suggest that a p75 antagonist can have neuro-protective effects on retinal ganglion [39]. In our study, MiMPC-conditioned medium was used to treat DRG cultures. The functional involvement of p75/NGFR will be tested in future studies by examining the effect of treatment with p75/NGFR inhibitors, for example, EVT901 [40], on neuritogenesis.

Our ELISA results show that NI-MiMPCs and NI-MSCs express BDNF, detectable in the conditioned media, although NI-MiMPCs are able to produce much higher levels of BDNF than NI-MSCs. However, conditioned media from MiMPCs and MSCs show comparable ability to encourage DRG neurite extension growth. Neurite extensions are denser when DRGs are cultured with

conditioned media taken from NI-MiMPCs and GM-MiMPCs, as well as GM-MSCs, as shown by Sholl analysis. Our initial thought was that the enhanced neurite growth resulted from the action of the NTFs, particularly the well-characterized BDNF, produced by the cells. We briefly investigated the effect of supplementing 20 ng/ml BDNF to basal medium and observed that the addition of

BDNF improved neurite extension lengths compared with controls (data not shown). However, when the actions of BDNF were blocked via the pan-Trk receptor inhibition drug GNF5837, neurite extension outgrowth was not completely abolished, and in the case of NI-MiMPC conditioned medium, were still significantly denser than those found in DRG control growth cultures. This
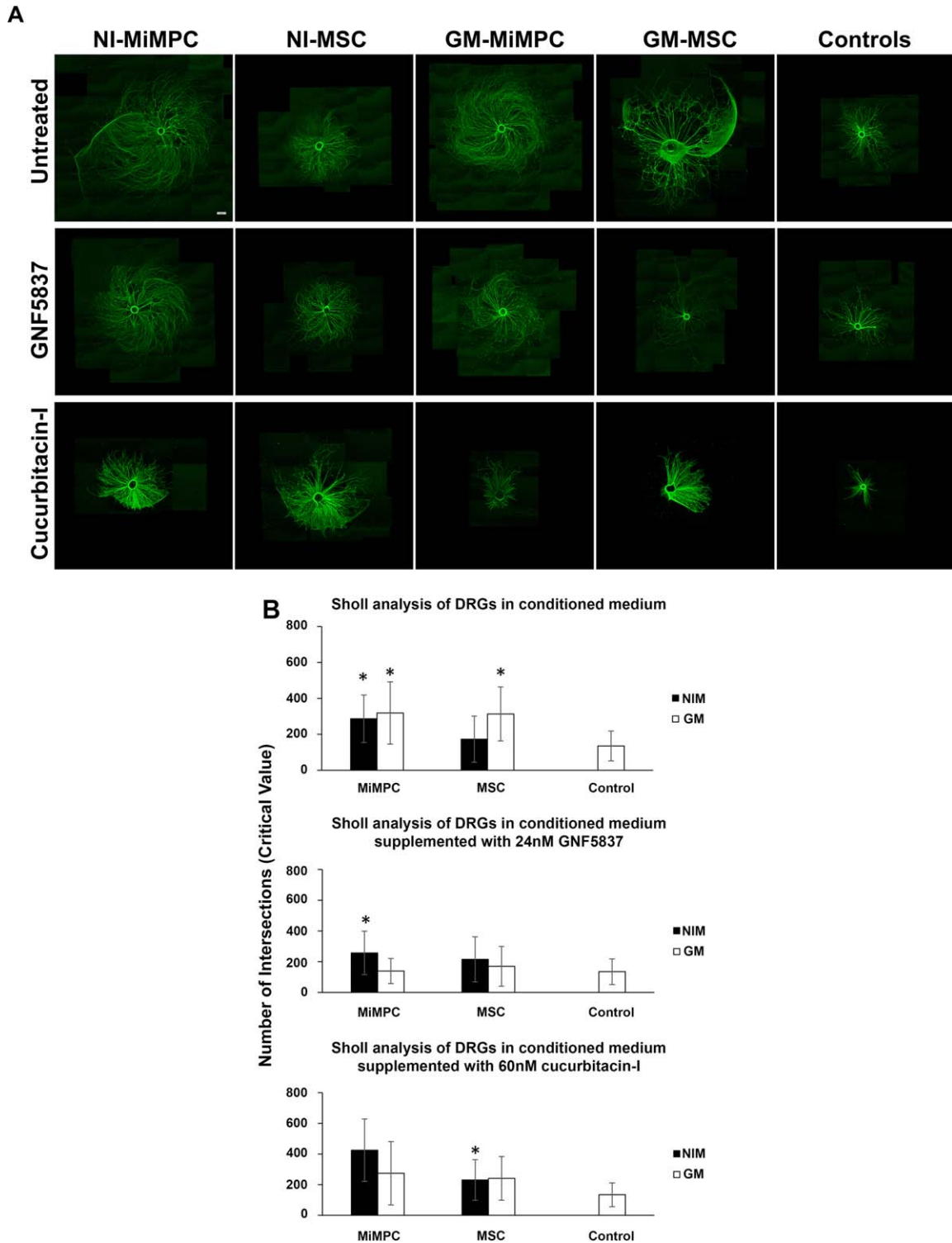

Figure 5.

finding strongly suggests that there may be another factor(s) present in the secretome of the induced MiMPCs and MSCs that aids neurite regeneration.

This unexpected result prompted us to investigate what other factors are produced by the cells that could be mediating the neurotrophic effect. Literature has shown that a varied host of cytokines and growth factors appear to have a positive effect on nerve regeneration [21, 24, 26, 27, 29, 41]. Our PCR array results show upregulation of the expression of a number of relevant cytokines, including IL-6, LIF, and osteopontin, the production of which is confirmed with ELISA performed on the cell-conditioned medium. We believe that aside from BDNF, these other cytokines may be responsible for the MiMPC and MSC mediated improvement of neurite growth observed in DRG cultures.

Osteonectin is a secreted matricellular protein that plays a role in bone mineralization by binding calcium to collagen [42]. Previous studies have shown that osteonectin can also play a role in promoting neural cell survival and initiating extension outgrowth [25, 26]. It has also been suggested that osteonectin and BDNF may work synergistically to promote neurite outgrowth. Although there is evidence to suggest that a specific receptor may exist, mediating osteonectin binding to cell surfaces in other tissues, such as smooth muscle cells and endothelial cells [25, 43, 44], this receptor has not yet been identified, and there is evidence to suggest that osteonectin only partially functions through the Trk receptors [27]. However, while both the MiMPCs and MSCs are capable of producing BDNF and osteonectin whether or not they have gone through neurotrophic induction, it seems that the positive effects of cell-conditioned medium on DRG outgrowth can be lessened, but not completely abolished, with the addition of GNF5837, a potent Trk-receptor inhibitor, for all conditioned medium groups except NI-MiMPCs. It is possible that dosage of both BDNF and osteonectin are important, or that osteonectin is operating through a yet unknown receptor pathway, which is likely as a major osteonectin-mediated signaling pathway has not yet been found [27]. Taking all this information together, it is likely that osteonectin production by the NI-MiMPCs is responsible for the increased neuritogenesis, and therefore, higher neurite extension density compared with controls, even in the presence of GNF5837. In our next studies, we plan to deplete osteonectin from the conditioned medium to assess whether osteonectin plays a synergistic role with BDNF in enhancing DRG neurite growth.

Osteopontin, a cell adhesion molecule that is expressed in a wide variety of cell types, has been implicated in cell survival and inflammatory regulation [45, 46]. A limited number of studies have suggested that osteopontin also plays a role in nerve regeneration, although the association is more likely to be with motor neuron outgrowth rather than sensory DRG neuron outgrowth [24, 46]. Clusterin is another commonly expressed glycoprotein found in most tissues, and various functional roles for clusterin have been implicated, including pathogenesis of Alzheimer's, and alleviation of peripheral neuropathy in rats [47, 48]. Interestingly, mRNA levels of clusterin were reported to increase after peripheral nerve injury, and as clusterin is involved in lipid recycling, it was suggested that the presence of this molecule at the site of injury aids Wallerian degeneration and Schwann cell proliferation [49, 50]. Meanwhile, clusterin may also signal through the megalin receptor, a pathway which has been shown in the DRG to selectively promote sensory neuron outgrowth [50, 51]. Although only sensory neurite outgrowth is assayed in the in vitro DRG model used here, the fact that the MiMPCs are capable of producing osteopontin as well as clusterin, suggests the potential application of MiMPCS for motor nerve injuries, further enhancing their clinical relevance.

It is well established that cytokines found in the IL-6 superfamily activate the Jak/STAT3 pathway, which is an important signaling pathway in neurite axon extension [33, 52]. We observed that upon pharmacologic blocking of Jak/STAT3 pathway activation, using cucurbitacin-I, the MiMPC/MSC-conditioned medium could not rescue the length of neurite extension, regardless of whether the conditioned medium was taken from induced cells or not. That only certain growth factors and cytokines, including IL-6, but not LIF, maintained their higher concentrations during and after the neuroinductive treatment period suggests that enhancement of neurite extensions found in conditioned medium cultures is a result of these cytokines, particularly IL-6, produced by the cells, by activating STAT3. Naturally, the possibility exists that LIF, also a potent cytokine, may exert a similar effect as IL-6 at a lower concentration [53]. However, as the equimolar potency of LIF versus IL-6 has been compared only on microvascular and endothelial cells [53], whether the two cytokines have similar effects on nerve regeneration remains to be assessed.

Topographical cues have long been found to affect cell adhesion, growth and differentiation [36, 54–56]. Multiple studies have shown the advantages of culturing DRGs on aligned surfaces, with improved adherence and axon elongation [34, 35, 56]. Therefore,

Figure 5. Immunofluorescent images and Sholl analysis of DRG neurite outgrowth upon treatment with conditioned media derived from neurotrophically induced MiMPCs and MSCs. **(A)**: Chick embryonic DRGs were cultured for 5 days in basal medium previously conditioned for 48 hours by NI-MiMPCs, NI-MSC, GM-MiMPCs, or GM-MSCs, or cultured in unconditioned basal medium (controls). For pan-Trk receptor inhibition, the inhibitor GNF5837 (24 nM final concentration) was added to each conditioned medium group and used to culture DRGs. Jak/STAT3 inhibition was achieved by the addition of the Jak/STAT3 inhibitor, cucurbitacin-I, at a final concentration of 60 nM, to each conditioned medium group and used to culture DRGs. Cultures exposed to conditioned media show substantial increase in size and complexity of neurite outgrowth compared with control groups. Cotreatment with GNF5837 did not result in apparent changes in neurite extension lengths. Cucurbitacin-I treatment drastically decreased the neurite extension lengths. Bar = 560 μm. **(B)**: Conditioned media from MiMPCs and MSCs are derived from (left) uninduced cells, and (right) induced cells. Sholl analysis measures the highest value of number of intersections where neurite branching is most dense (critical value). Controls consisted of basal medium alone that was not unconditioned by cells. Sholl analysis was carried out on DRG cultures exposed to conditioned media alone (top row), or conditioned media in the presence of the pan-Trk inhibitor, GNF5837 (24 nM final concentration) (middle row), or the Jak/STAT3 inhibitor, cucurbitacin-I (60 nM final concentration). Sholl analysis showed that conditioned medium from uninduced MiMPCs and MSCs significantly increased DRG neurite branching complexity compared with controls. Conditioned medium from NI-MiMPCs significantly increased DRG neurite branching complexity even in the presence of GNF5837. Conditioned medium from induced MSCs were unable to enhance branching complexity, and could not rescue neuritogenesis in the presence of GNF5837. The presence of cucurbitacin-I in conditioned medium decreased the number of neurite extensions in all conditioned medium except for that collected from induced MSCs. *, $p < .05$, indicating significant differences in complexity, compared via Games-Howell tests. At least 10 images per group were quantified via Sholl analysis. Abbreviations: DRG, dorsal root ganglia; GM-MiMPCs, control MiMPCs; GM-MSCs, control MSCs; NI-MSCs, neurotrophically induced-MSCs; NI-MiMPCs, neurotrophically induced-MiMPCs.
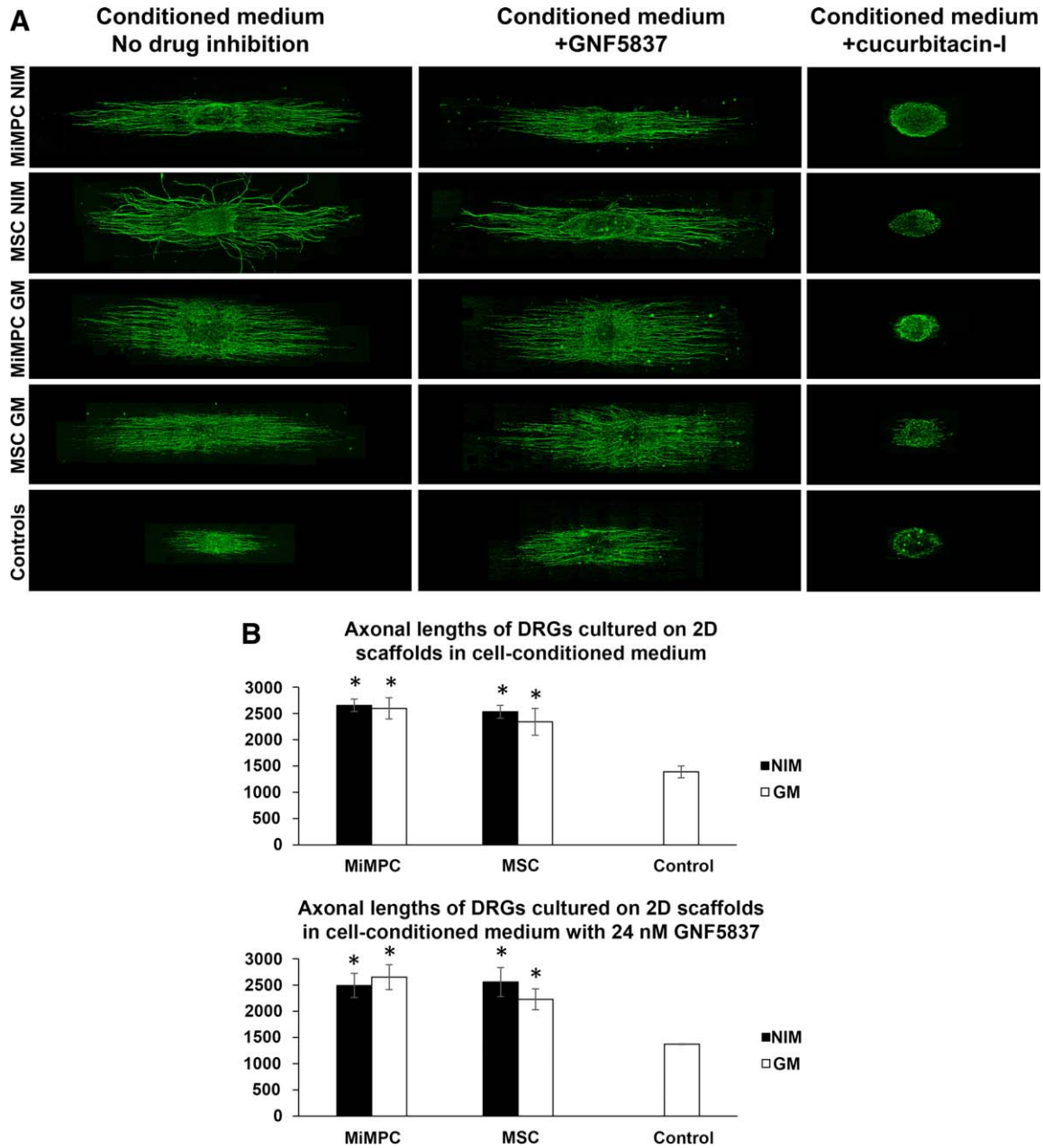
Figure 6. Morphological effect of MiMPCs and MSCs on neurite outgrowth in DRGs grown on electrospun nanofibrous scaffolds via image analysis and measurements by NIH ImageJ. **(A)**: DRGs were cultured on aligned nanofibrous scaffolds prepared as described in Materials and Methods, using media conditioned by induced (NI) and noninduced (GM) MiMPCs and MSCs, with or without cotreatment with the pan Trk-receptor inhibitor, GNF5837 (24 nM), or the Jak/Stat inhibitor, cucurbitacin-I (60 nM). No observable difference in neurite extension lengths was seen, compared with cultures without GNF5837 cotreatment. On the other hand, cucurbitacin-I cotreatment resulted in substantial decrease in in neurite extension length, compared with controls or any other group. Neurite extension lengths were measured with ImageJ. Bar = 800 μm. **(B)**: Neurite extension outgrowth was traced using NIH ImageJ. DRGs were cultured on aligned scaffolds with conditioned media collected from NI- and GM- MiMPCs and MSCs. Results on neurite outgrowth lengths indicate that exposure to NI- and GM- MiMPC and MSC conditioned media improved neurite outgrowth compared with controls, and the addition of Trk-receptor inhibitor (+GNF5837) did not impede length of neurite extension. *, $p < .05$, denotes statistically significant difference compared with both controls. At least 10 axons were measured per group over an $n = 3$. Abbreviations: GM, growth medium; MiMPCs, induced mesenchymal progenitor cells; MSCs, mesenchymal stem cells; NIM, neurotrophic induction medium.

we chose such favorable environments consisting of an aligned nanotopographical surface for DRG cultures to examine the potential advantage of combining MiMPC/MSC conditioned medium with scaffolds on neurite outgrowth. In Figure 6, length measurements showed enhanced DRG axon elongation in conditioned medium cultures compared with controls, although there were no significant differences between the various conditioned medium groups. This result could be due to the fact that NI-treated MiMPCs did not proliferate as well as NI-MSCs. Thus, while MiMPCs are capable of producing more neurotrophins and

cytokines per cell, the overall reduced cell count compared with that of MSCs results in a comparable level of neurotrophins produced per population of cells, and lack of significant difference in axon length between the two groups. Another possibility is that a saturated concentration of neurotrophins has already been reached or exceeded in the experimental system, that is, a "maximum" concentration of neurotrophins and cytokines at which an observable increase in axon length occurs.

All experiments were performed with MiMPCs differentiated from human MSC-derived iPSCs, and the results were compared with those achieved by human MSCs. Sholl analysis on DRGs cultured in conditioned medium on tissue culture plastic, and length measurements taken from DRGs cultured on 2D aligned scaffolds showed enhanced branching and length compared with controls. Our findings show that MiMPCs can provide similar advantages as MSCs, which makes MiMPCs clinically applicable, and can serve as a less invasive and, more importantly, sustainable therapeutic method.

While our findings suggest the potential neurotrophic capabilities of MiMPCs, there are a number of caveats. First, it is noteworthy that MiMPCs are less hardy than MSCs, namely, MiMPCs showed lower viability in the serum-free, neuro-inductive medium. In the literature, induction media treatments are achieved with a 0%–2% serum content [4, 5, 57], while in our investigation, serum content of NIM for MiMPCs was elevated to 5%, which we believe did not significantly compromise production of NTFs. Second, chick embryonic DRGs were used as an in vitro model for functional bioassay of NTFs production by NI-MiMPCs. While this is a well-established system to study neurotrophic effects, it will be necessary to assess NI-MiMPC NTF production and function using mammalian, and preferably in vivo, system as well.

current research with MiMPCs have focused on differentiation and potential cellular therapy candidates for nerve regeneration, however, in future studies, it may be beneficial to characterize in greater detail the full scope of differences between MiMPCs and MSCs or Schwann cells in terms of secretome and mechanisms behind these differences. Our current experiments did not include Schwann cells for the simple fact that our goal was not to replace the patient's native Schwann cell, but rather, to identify a possible substitute for the MSC, which is by far more ubiquitous in regenerative medicine research, and likeness to the MSC will offer more wide-reaching avenues of future studies. With these studies, we hope to critically examine the applicability of MiMPCs as an alternative cell type to autologous Schwann cells or MSCs to aid the healing of peripheral nerve injuries, particularly those resulting from trauma.

AUTHOR CONTRIBUTIONS

R.M.B., A.X.S., and R.S.T.: manuscript writing, final approval of the manuscript

CONCLUSION

In this study, we have determined that MiMPCs support neurite sprouting and axon elongation through the secretion of neurotrophic factors and are a viable alternative to MSCs for nerve regeneration. Our next work will focus on in vivo studies, designed to determine if combining MiMPCs in a bioscaffold will be beneficial for repairing traumatic sciatic nerve injury in a rat model. As both length and branching pattern were similar upon exposure of DRGs to NI-MiMPCs and GM-MiMPCs in vitro, our in vivo study will use GM-MiMPCs for practicality and ease of cell preparation. Our

DISCLOSURE OF POTENTIAL CONFLICTS OF INTEREST

The authors indicated no potential conflicts of interests.

NOTE ADDED IN PROOF

This article was published online on 07 December 2017. Minor edits have been made that do not affect data. This notice is included in the online and print versions to indicate that both have been corrected 28 December 2017.

REFERENCES

1 Fairbairn NG, Meppelink AM, Ng-Glazier J et al. Augmenting peripheral nerve regeneration using stem cells: A review of current opinion. World J Stem Cells 2015;7:11–26.

2 Wolford LM, Stevao ELL. Considerations in nerve repair. Proc (Bayl Univ Med Cent) 2003;16:152–156.

3 Mosahebi A, Fuller P, Wiberg M et al. Effect of allogeneic Schwann cell transplantation on peripheral nerve regeneration. Exp Neurol 2002;173:213–223.

4 Keilhoff G, Stang F, Goihl A et al. Transdifferentiated mesenchymal stem cells as alternative therapy in supporting nerve regeneration and myelination. Cell Mol Neurobiol 2006;26:1233–1250.

5 Jackson WM, Alexander PG, Bulken-Hoover JD et al. Mesenchymal progenitor cells derived

from traumatized muscle enhance neurite growth. J Tissue Eng Regen Med 2013;7:443–451.

6 Diederichs S, Tuan RS. Functional comparison of human induced pluripotent stem cell-derived mesenchymal cells and bone marrow-derived mesenchymal stromal cells from the same donor. Stem Cells Dev 2014;23:1594–1610.

7 Nishi R. Autonomic and sensory neuron cultures. In: Marianne B-F, ed. Methods in Cell Biology, Chapter 13. New York: Academic Press, 1996;51:249–263.

8 Albaugh P, Fan Y, Mi Y et al. Discovery of GNF-5837, a selective TRK inhibitor with efficacy in rodent cancer tumor models. ACS Med Chem Lett 2012;3:140–145.

9 Blaskovich MA, Sun J, Cantor A et al. Discovery of JSI-124 (cucurbitacin I), a selective Janus kinase/signal transducer and activator of transcription 3 signaling pathway inhibitor with potent antitumor activity

against human and murine cancer cells in mice. Cancer Res 2003;63:1270–1279.

10 Schindelin J, Arganda-Carreras I, Frise E et al. Fiji: An open-source platform for biological image analysis. Nat Methods 2012;9:676. 10.1038/nmeth.2019.

11 Ferreira TA, Blackman AV, Oyrer J et al. Neuronal morphometry directly from bitmap images. Nat Methods 2014;11:982–984.

12 Lin H, Zhang D, Alexander PG et al. Application of visible light-based projection stereolithography for live cell-scaffold fabrication with designed architecture. Biomaterials 2013;34:331–339.

13 Fairbanks BD, Schwartz MP, Bowman CN et al. Photoinitiated polymerization of PEG-diacrylate with lithium phenyl-2,4,6-trimethylbenzoylphosphinate: Polymerization rate and cytocompatibility. Biomaterials 2009; 30:6702–6707.

14 Yang G, Lin H, Rothrauff BB et al. Multi-layered polycaprolactone/gelatin fiber-hydrogel composite for tendon tissue engineering. Acta Biomater 2016;35:68–76.

15 Liedtke W, Edelmann W, Bieri PL et al. GFAP is necessary for the integrity of CNS white matter architecture and long-term maintenance of myelination. Neuron 1996;17:607–615.

16 Bentley CA, Lee K-F. p75 is important for axon growth and Schwann cell migration during development. J Neurosci 2000;20:7706–7715.

17 Abreu RS, Penalva LO, Marcotte EM et al. Global signatures of protein and mRNA expression levels. Mol Biosyst 2009;5:1512–1526.

18 Koussounadis A, Langdon SP, Um IH et al. Relationship between differentially expressed mRNA and mRNA-protein correlations in a xenograft model system. Sci Rep 2015;5:10775.

19 Vogel C, Marcotte EM. Insights into the regulation of protein abundance from proteomic and transcriptomic analyses. Nat Rev Genet 2012;13:227–232.

20 Hirota H, Kiyama H, Kishimoto T et al. Accelerated nerve regeneration in mice by upregulated expression of interleukin (IL) 6 and IL-6 receptor after trauma. J Exp Med 1996;183:2627–2634.

21 Leibinger M, Muller A, Gobrecht P et al. Interleukin-6 contributes to CNS axon regeneration upon inflammatory stimulation. Cell Death Dis 2013;4:e609.

22 Frostick SP, Yin Q, Kemp GJ. Schwann cells, neurotrophic factors, and peripheral nerve regeneration. Microsurgery 1998;18:397–405.

23 McKay HA, Wiberg M, Terenghi G. Exogenous leukaemia inhibitory factor enhances nerve regeneration after late secondary repair using a bioartificial nerve conduit. Br J Plast Surg 2003;56:444–450.

24 Wright MC, Mi R, Connor E et al. Novel roles for osteopontin and clusterin in peripheral motor and sensory axon regeneration. J Neurosci 2014;34:1689–1700.

25 Bampton ETW, Ma CH, Tolkovsky AM et al. Osteonectin is a Schwann cell-secreted factor that promotes retinal ganglion cell survival and process outgrowth. Eur J Neurosci 2005;21:2611–2623.

26 Ma CHE, Palmer A, Taylor JSH. Synergistic effects of osteonectin and NGF in promoting survival and neurite outgrowth of superior cervical ganglion neurons. Brain Res 2009;1289:1–13.

27 Ma CHE, Bampton ETW, Evans MJ et al. Synergistic effects of osteonectin and brain-derived neurotrophic factor on axotomized retinal ganglion cells neurite outgrowth via the mitogen-activated protein kinase-extracellular signal-regulated kinase1/2 pathways. Neuroscience 2010;165:463–474.

28 Sholl DA. Dendritic organization in the neurons of the visual and motor cortices of the cat. J Anat 1953;87:387–406.

29 Yang P, Wen H, Ou S et al. IL-6 promotes regeneration and functional recovery after cortical spinal tract injury by reactivating intrinsic growth program of neurons and enhancing synapse formation. Exp Neurol 2012;236:19–27.

30 Lin G, Zhang H, Sun F et al. Brain-derived neurotrophic factor promotes nerve regeneration by activating the JAK/STAT pathway in Schwann cells. Transl Androl Urol 2016;5:167–175.

31 Bella AJ, Lin G, Tantiwongse K et al. Brain-derived neurotrophic factor (BDNF) acts primarily via the JAK/STAT pathway to promote neurite growth in the major pelvic ganglion of the rat: Part I. J Sex Med 2006;3:815–820.

32 Yadav A, Kalita A, Dhillon S et al. JAK/STAT3 pathway is involved in survival of neurons in response to insulin-like growth factor and negatively regulated by suppressor of cytokine signaling-3. J Biol Chem 2005;280:31830–31840.

33 Elsaeidi F, Bemben MA, Zhao X et al. Jak/Stat signaling stimulates zebrafish optic nerve regeneration and overcomes the inhibitory actions of Socs3 and Sfpq. J. Neurosci 2014;34:2632–2644.

34 Zamani F, Amani-Tehran M, Latifi M et al. The influence of surface nanoroughness of electrospun PLGA nanofibrous scaffold on nerve cell adhesion and proliferation. J Mater Sci Mater Med 2013;24:1551–1560.

35 Brunetti V, Maiorano G, Rizzello L et al. Neurons sense nanoscale roughness with nanometer sensitivity. Proc Natl Acad Sci USA 2010;107:6264–6269.

36 Hoffman-Kim D, Mitchel JA, Bellamkonda RV. Topography, cell response, and nerve regeneration. Annu Rev Biomed Eng 2010;12:203–231.

37 Haase G, Pettmann B, Raoul C et al. Signalling by death receptors in the nervous system. Curr Opin Neurobiol 2008;18:284–291.

38 Bamji SX, Majdan M, Pozniak CD et al. The p75 neurotrophin receptor mediates neuronal apoptosis and is essential for naturally occurring sympathetic neuron death. J Cell Biol 1998;140:911–923.

39 Bai Y, Dergham P, Nedev H et al. Chronic and acute models of retinal neurodegeneration TrkA activity are neuroprotective whereas p75NTR activity is neurotoxic through a paracrine mechanism. J Biol Chem 2010;285:39392–39400.

40 Delbary-Gossart S, Lee S, Baroni M et al. A novel inhibitor of p75-neurotrophin receptor improves functional outcomes in two models of traumatic brain injury. Brain 2016;139:1762–1782.

41 Ogai K, Kuwana A, Hisano S et al. Upregulation of leukemia inhibitory factor (LIF) during the early stage of optic nerve regeneration in zebrafish. PLoS One 2014;9:e106010.

42 Rosset EM, Bradshaw AD. SPARC/osteonectin in mineralized tissue. Matrix Biol 2016;52–54:78–87.

43 Motamed K, Funk SE, Koyama H et al. Inhibition of PDGF-stimulated and matrix-mediated proliferation of human vascular smooth muscle cells by SPARC is independent of changes in cell shape or cyclin-dependent kinase inhibitors. J Cell Biochem 2002;84:759–771.

44 Yost JC, Sage EH. Specific interaction of SPARC with endothelial cells is mediated through a carboxyl-terminal sequence containing a calcium-binding EF hand. J Biol Chem 1993;268:25790–25796.

45 Denhardt DT, Noda M, O'Regan AW et al. Osteopontin as a means to cope with environmental insults: Regulation of inflammation, tissue remodeling, and cell survival. J Clin Invest 2001;107:1055–1061.

46 Hashimoto M, Sun D, Rittling SR et al. Osteopontin-deficient mice exhibit less inflammation, greater tissue damage, and impaired locomotor recovery after spinal cord injury compared with wild-type controls. J Neurosci 2007;27:3603–3611.

47 Dati G, Quattrini A, Bernasconi L et al. Beneficial effects of r-h-CLU on disease severity in different animal models of peripheral neuropathies. J Neuroimmunol 2007;190:8–17.

48 Bonnard A-S, Chan P, Fontaine M. Expression of clusterin and C4 mRNA during rat peripheral nerve regeneration. Immunopharmacology 1997;38:81–86.

49 Liu L, Svensson M, Aldskogius H. Clusterin upregulation following rubrospinal tract lesion in the adult rat. Exp Neurol 1999;157:69–76.

50 Fitzgerald M, Nairn P, Bartlett CA et al. Metallothionein-IIA promotes neurite growth via the megalin receptor. Exp Brain Res 2007;183:171–180.

51 Fleming CE, Mar FM, Franquinho F et al. Transthyretin internalization by sensory meurons Is megalin mediated and necessary for Its neuritogenic activity. J Neurosci 2009;29:3220–3232.

52 Heinrich PC, Behrmann I, Müller-Newen G et al. Interleukin-6-type cytokine signalling through the gp130/Jak/STAT pathway. Biochem J 1998;334:297–314.

53 Günthert U, Birchmeier W. Attempts to Understand Metastasis Formation II: Regulatory Factors. Berlin Heidelberg: Springer, 2012.

54 Boroujeni SM, Mashayekhan S, Vakilian S et al. The synergistic effect of surface topography and sustained release of TGF-β1 on myogenic differentiation of human mesenchymal stem cells. J Biomed Mater Res A 2016;104:1610–1621.

55 Yim EKF, Pang SW, Leong KW. Synthetic nanostructures inducing differentiation of human mesenchymal stem cells into neuronal lineage. Exp Cell Res 2007;313:1820–1829.

56 Patel S, Kurpinski K, Quigley R et al. Bioactive nanofibers: Synergistic effects of nanotopography and chemical signaling on cell guidance. Nano Lett 2007;7:2122–2128.

57 Sadan O, Shemesh N, Barzilay R et al. Mesenchymal stem cells induced to secrete neurotrophic factors attenuate quinolinic acid toxicity: A potential therapy for Huntington's disease. Exp Neurol 2012;234:417–427.

See www.StemCellsTM.com for supporting information available online.